Progress In Electromagnetics Research C, Vol. 51, 95–101, 2014

RCS Reduction of Patch Array Antenna by Complementary Split-Ring Resonators Structure

Jun Zheng[1, 2], Shaojun Fang[1], Yongtao Jia[3, *], and Ying Liu[3]

Abstract—In this paper, a new approach for the radar cross section (RCS) reduction of patch array antenna is proposed. Complementary split-ring resonators (CSRRs) are etched on the ground of the proposed patch antenna array. A conventional 1×4 patch antenna array is designed with the central frequency of 5.0 GHz. The monostatic RCS of the patch antenna array with CSRRs can be reduced as much as 14 dB compared to that of the conventional array while maintaining almost the same radiation characters. For the case of φ-polarized incident wave, the RCS has been reduced in the angular range of $-90^\circ \leq \theta \leq +90^\circ$ in xoz-plane and this angular range is usually less than $\pm 45^\circ$ when using conventional methods of RCS reduction.

1. INTRODUCTION

In recent years, with the rapid development of detection and stealth technologies, radar cross section (RCS) reduction of antennas has been a serious problem in weapon platforms because antennas can be the dominant scatters for low RCS platforms [1] and more and more attention has been paid to antenna scattering. Antenna is a special scatter whose radiation characters and RCS should be considered simultaneously [2]. Therefore, the methods used for other scatters, such as shaping and covering radar absorbing materials (RAM), can't be simply applied to RCS reduction of antennas.

Some methods are reported for RCS reduction of antennas, such as using fractal structure [3], modifying the antenna structure [4, 5], and using bionics principle [6]. Frequency selective surface (FSS) [7], works well when reducing out-band RCS of antenna, but it doesn't fit for the case of in-band RCS reduction. For the case of reducing in-band RCS of antenna, electromagnetic band-gap (EBG) structure is utilized in [8]. Although the backward RCS of the patch array antenna with EBG can be reduced as much as 10 dB compared to that of the conventional array antenna, its directivity is 2 dB lower. Besides, the angular range in which the RCS has been reduced is usually less than $\pm 45^\circ$ in the reported publications.

The structure of SRR and CSRR is widely used in band-notched antenna [9–11], antenna miniaturization [12], band-pass filter [13], and so on. Nevertheless, up to now few papers for RCS reduction using CSRR have been reported. In this paper, a new compact CSRR structure is designed and utilized for in-band RCS reduction of patch array antenna. The backward RCS has been reduced significantly in the angular ranges of $-90^\circ \leq \theta \leq +90^\circ$, and there are barely other methods reported can that achieve this goal without degradation of antenna performance.

Received 5 May 2014, Accepted 9 June 2014, Scheduled 19 June 2014
* Corresponding author: Yongtao Jia (jiazong0629@163.com).
[1] School of Information Science and Technology, Dalian Maritime University, Dalian 116026, China. [2] Beijing Electro-mechanical Engineering Institute, Beijing 100074, China. [3] National Laboratory of Science and Technology on Antennas and Microwaves, Xidian University, Xi'an 710071, China.

2. DESIGN AND ANALYSIS

2.1. Complementary Split-Ring Resonator

Split-ring resonator (SRR) with only electric excitation or magnetic excitation shows the band-stop characteristics at its resonance [14]. So according to the Babinet Principle [2], the CSRR will have the band-pass characteristics. According to [15], CSRR can be intrinsically described by simple LC circuits

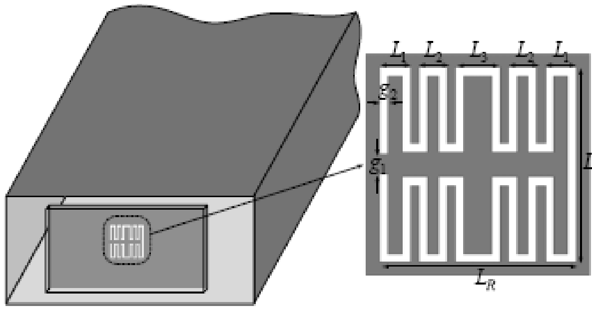

Figure 1. Simulative demonstration and geometry of the compact CSRR.

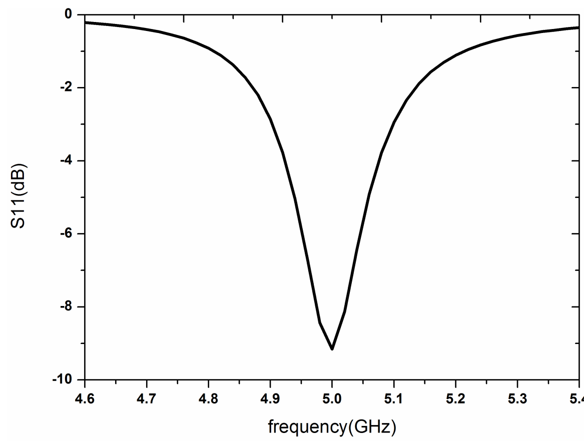

Figure 2. Simulated S_{11} of compact CSRR in a rectangular waveguide.

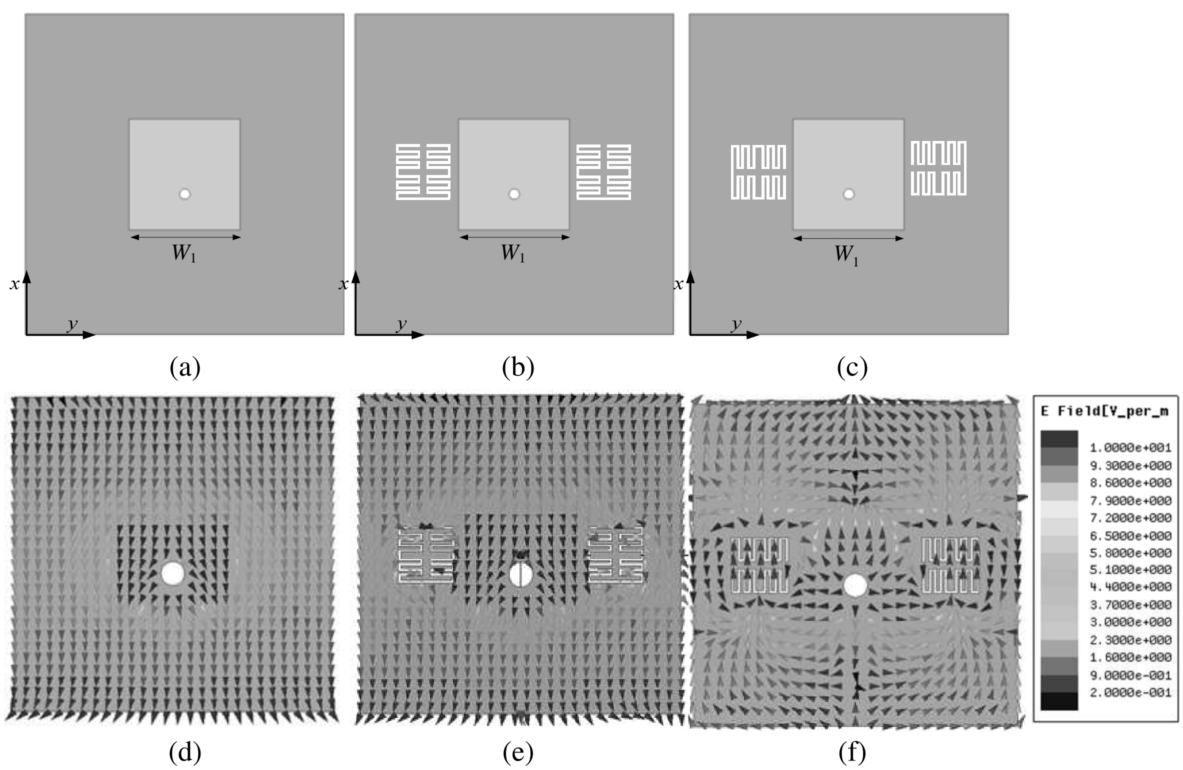

Figure 3. Geometry of the (a) antenna 1, (b) antenna 2, and (c) antenna 3, and the current distribution on the ground of (d) antenna 1, (e) antenna 2, and (f) antenna 3.

with a resonant frequency

$$f = \frac{1}{2\pi\sqrt{LcCc}} \tag{1}$$

where Lc and Cc are the inductance and capacitance of the CSRR.

In order to miniaturize the size of CSRR, a compact CSRR resonate at 5 GHz is designed and simulated. The sketch of the geometry and simulative demonstration of the compact CSRR is given in Fig. 1. The parameters are as following: $L_R = 7$ mm, $g_1 = 0.7$ mm, $g_2 = 0.3$ mm, $L_1 = 1.1$ mm, $L_2 = 1$ mm, $L_3 = 1.6$ mm, and the thickness of the substrate covering the CSRR is 1 mm with the relative permittivity of 4.4. The rectangular waveguide is used to simulate the S-parameters of the CSRR structure by the commercial software High Frequency Structure Simulator (HFSS). It can be obtained from Fig. 2 that the band-pass characteristics of the designed compact CSRR appears at 5 GHz and this feature is used to design a low RCS patch antenna array in Section 3.

In order to study the influence of CSRR to the radiation characteristics of microstrip antennas, several simulations are conducted. The microstrip antenna with and without CSRRs are shown in Figs. 3(a), (b), and (c), separately. The parameter of the square patch is $W_1 = 13.72$ mm works and width of the metallic ground is 30 mm. The microstrip antenna without CSRRs is designed at 5 GHz. The currents on the grounds of the antennas without CSRRs and with CSRRs of different orientations are given in Figs. 3(d), (e), and (f), respectively. When the opening end of CSRRs is along the x-axis, the current distribution almost keeps unchanged with that of the conventional antenna, and when along y-axis, the current distribution is completely different. The S_{11} of the three antennas are given in Fig. 4. As expected, antenna 2 (Fig. 3(e)) has the same S-parameters with antenna 1 (Fig. 3(d)), while the resonance frequency of antenna 3 (Fig. 3(f)) is shifted. So the CSRRs can be used without destroying the radiation when the opening end is along the direction of the currents on the ground.

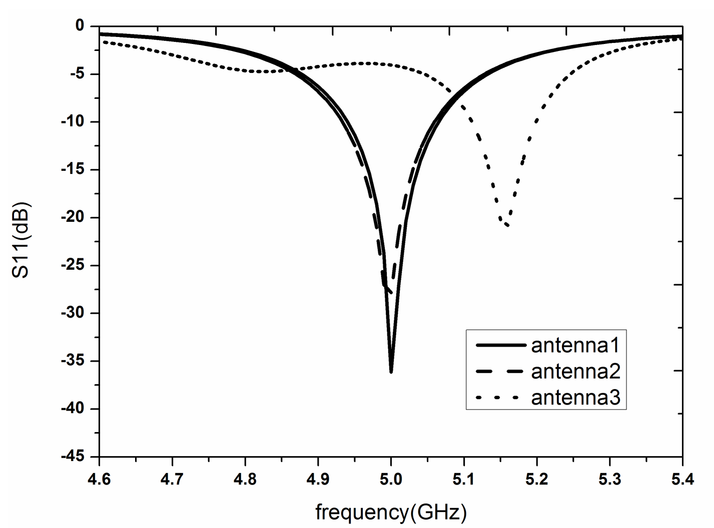

Figure 4. Simulated S_{11} of the microstrip antennas.

2.2. Low RCS Patch Array Antenna

Figure 5 shows a 1×4 patch array antenna fed by coaxial probes, which works at the central frequency of 5 GHz. The parameters of the patch array antenna are as following: $L_a = 120$ mm, $W_a = 30$ mm, $L = 13.72$ mm, $W = 13.72$ mm, and $a = 16.28$ mm. The thickness of the substrate is 1 mm and its relative permittivity is 4.4. Fig. 6(a) shows the geometry of the ground of patch antenna array with CSRRs and $L_{g1} = 0.9$ mm, $L_{g2} = 0.5$ mm. The size of the CSRR is the same as that designed and simulated in Fig. 2. Fig. 6(b) shows the photograph of the fabricated patch array antennas.

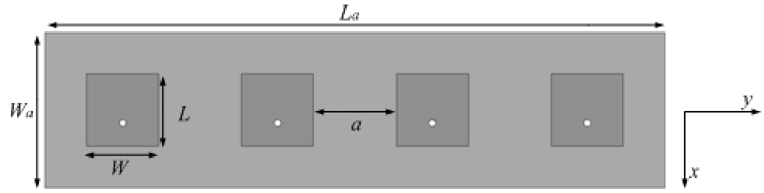

Figure 5. 1×4 patch antenna array.

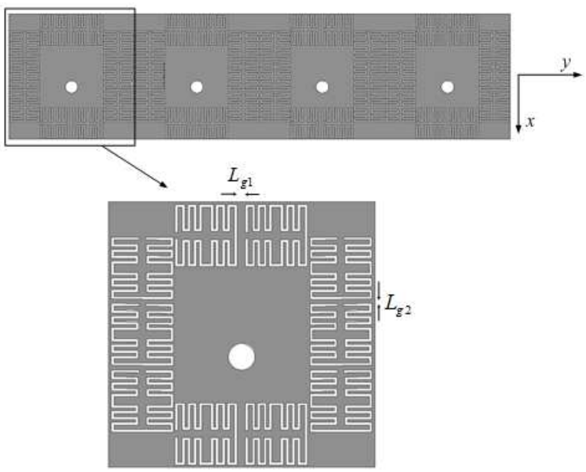

(a)

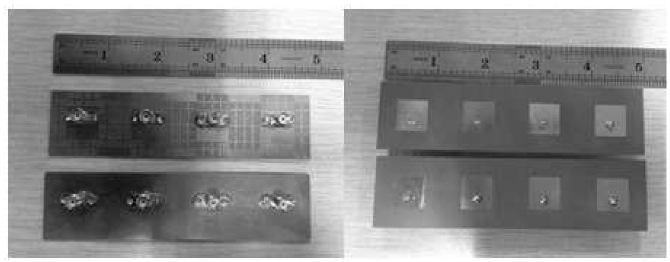

(b)

Figure 6. (a) Geometry of the patch antenna array with CSRRs etched on the ground. (b) Photograph of the patch array antennas with and without CSRRs.

3. RESULTS

Figure 7 gives the simulated and measured S_{11} of two patch array antennas with and without CSRRs, from which it can be seen that the two patch array antennas have the same resonant frequency and simulation results are in agreement with the experimental results. In Fig. 8, the gain of the antenna

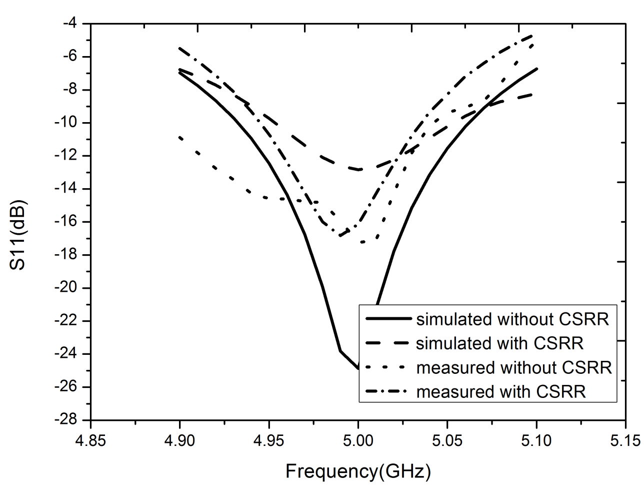

Figure 7. Comparison of simulated and measured S_{11} of the array antennas with and without CSRRs.

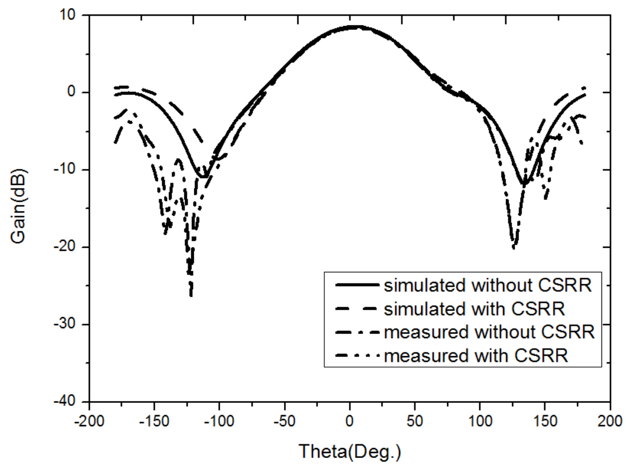

(a)

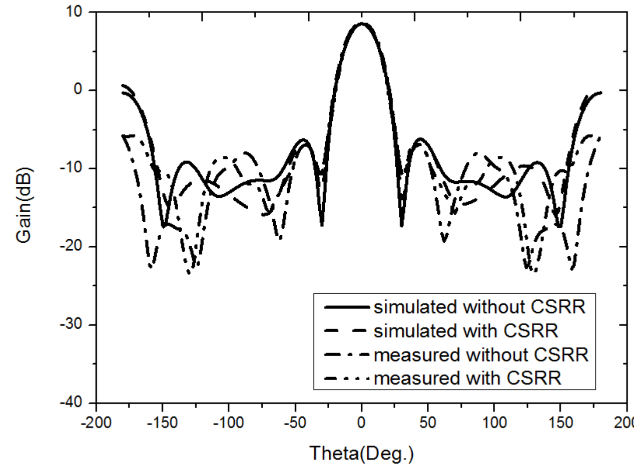

(b)

Figure 8. Comparison of radiation pattern of the array antennas with and without CSRRs. (a) *xoz*-plane. (b) *yoz*-plane.

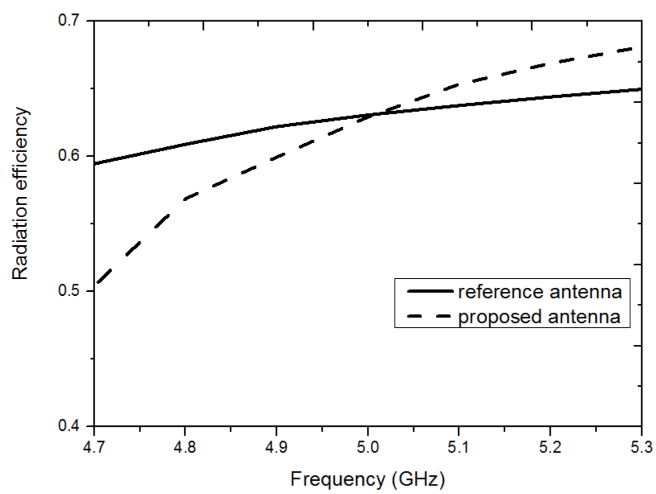

Figure 9. Comparison of the radiation efficiency of the reference antenna and proposed antenna.

with CSRRs is 8.58 dB which is just 0.03 dB lower than the gain of the conventional antenna. The radiation patterns of the two antennas are similar both in *xoz*-plane and *yoz*-plane and the radiation characters of the patch array antenna with CSRRs don't degrade compared to that without CSRRs. The back lobe of the proposed antenna doesn't degrade although the CSRRs are etched around the patch on the metallic ground. That's because the orientation of the CSRRs are well designed and the CSRRs are not excited by the electromagnetic field of the proposed antenna itself. Fig. 9 shows the radiation efficiency of the reference antenna and proposed antenna. It can be seen that the efficiency of the two antennas are nearly the same at 5 GHz.

Figure 10 shows the monostatic RCS of the two patch array antennas in *xoz*-plane and *yoz*-plane with φ-polarized incident wave. In *xoz*-plane, the monostatic RCS has been significantly reduced in the angular ranges of $-90^\circ \leq \theta \leq +90^\circ$, and the RCS in the direction normal to the antenna is reduced by 14.3 dB. For the case of *yoz*-plane, the monostatic RCS is reduced in the angular ranges of $-35^\circ \leq \theta \leq +35^\circ$, $-50^\circ \leq \theta \leq -75^\circ$, and $+50^\circ \leq \theta \leq +75^\circ$, and the RCS in the direction normal to the antenna is reduced by 4.7 dB. The effect of RCS reduction in *xoz*-plane is better than that in *yoz*-plane. The reason for this phenomenon is that the CSRRs with different directions vary in numbers

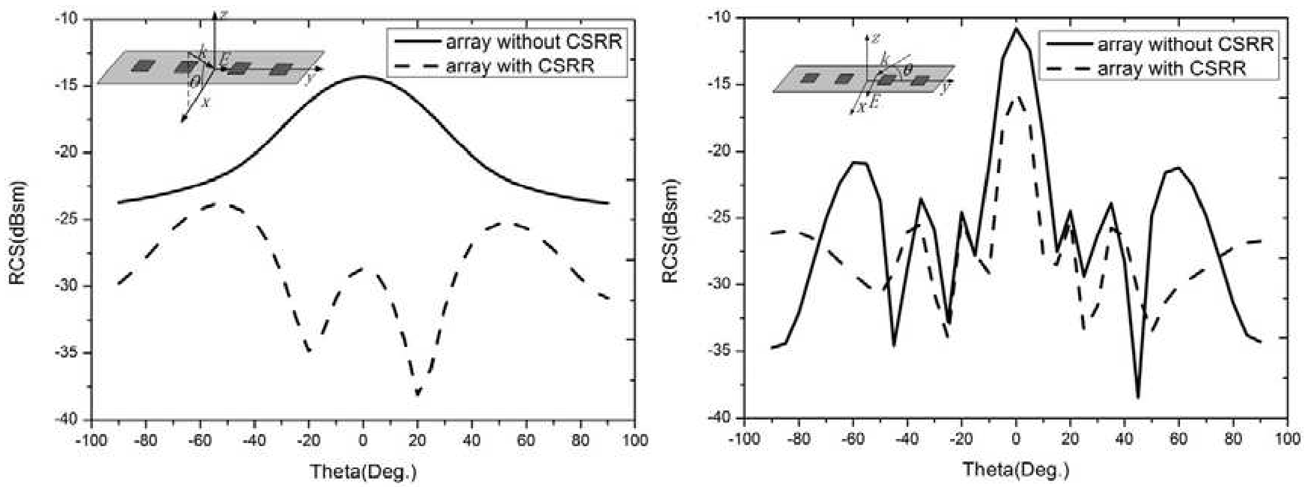

(a) (b)

Figure 10. Comparison of monostatic RCS of the two array antennas with φ-polarized incident wave. (a) xoz-plane. (b) yoz-plane.

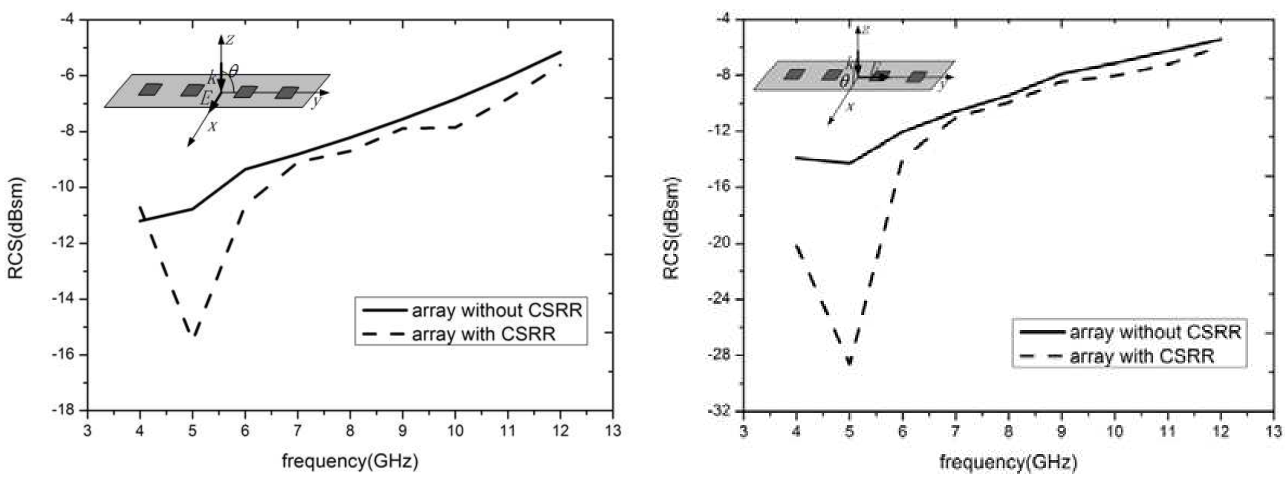

(a) (b)

Figure 11. Comparison of monostatic RCS of the two array antennas with (a) x-polarized incident wave, (b) y-polarized incident wave.

and arrangement manners (Fig. 6(b)).

The monostatic RCS in the band of 4.0–12.0 GHz with x-polarized and y-polarized incident waves is given in Fig. 11(a) and Fig. 11(b), respectively. The direction of incident waves is parallel to z-axis. In the whole band, the RCS of the patch antenna array with CSRRs is lower than that of the antenna without CSRRs.

4. CONCLUSION

The CSRRs are used for reducing the RCS of patch array antenna. A 1×4 patch array antenna with CSRRs etched on the antenna ground, as well as one without CSRRs, is designed, simulated and measured. The results show that the RCS can be significantly reduced when the CSRR is designed in the band of antenna and that the backward RCS reduction in xoz-plane over the angular range is $-90^\circ \leq \theta \leq +90^\circ$. Meanwhile, there is almost no degradation in antenna performance.

ACKNOWLEDGMENT

This work is supported by Program for New Century Excellent Talents in University (NCET-11-0690) and by the National Natural Science Foundation of China (No. 61372001).

REFERENCES

1. Knott, E. F., *Radar Cross Section*, 2nd edition, SciTech, Raleigh, NC, 2004.
2. Balanis, C. A. *Antenna Theory: Analysis and Design*, John Wiley & Sons, 2012.
3. Liu, Y., S.-X. Gong, and H.-B. Zhang, "A novel fractal slot microstrip antenna with low RCS," *IEEE Antennas and Propagation Society International Symposium*, 2603–2606, 2006.
4. Jia, Y., Y. Liu, S.-X. Gong, T. Hong, and D. Yu, "Printed UWB end-fire Vivaldi antenna with low RCS," *Progress In Electromagnetics Research Letters*, Vol. 37, 11–20, 2013.
5. Hong, T., S.-X. Gong, W. Jiang, Y.-X. Xu, and X. Wang, "A novel ultra-wide band antenna with reduced radar cross section," *Progress In Electromagnetics Research*, Vol. 96, 299–308, 2009.
6. Jiang, W., Y. Liu, S.-X. Gong, and T. Hong, "Application of bionics in antenna radar cross section reduction," *IEEE Antennas and Wireless Propagation Letters*, Vol. 8, 1275–1278, 2009.
7. Genovesi, S., F. Costa, and A. Monorchio, "Low-profile array with reduced radar cross section by using hybrid frequency selective surfaces," *IEEE Transactions on Antennas and Propagation*, Vol. 60, No. 5, 2327–2335, 2012.
8. Zhang, J. J., J.-H. Wang, M.-E. Chen, and Z. Zhang, "RCS reduction of patch array antenna by electromagnetic band-gap structure," *IEEE Antennas and Wireless Propagation Letters*, Vol. 11, 1048–1051, 2010.
9. Jiang, D., "Compact dual-band-notched UWB planar monopole antenna with modified CSRR," *Electronics Letters*, Vol. 48, No. 20, 1250–1252, 2012.
10. Lee, Y., "A compact microstrip antenna with improved bandwidth using complementary split-ring resonator (CSRR) loading," *Antennas and Propagation Society International Symposium*, 5431–5434, 2007.
11. Sun, H., G. Wen, Y. Huang, J. Li, W. Zhu, and L. Si, "Tunable band notch filters by manipulating coupling of split ring resonators," *Applied Optics*, Vol. 52, No. 31, 7517–7522, 2013.
12. Li, Y., W. Li, and Q. Ye, "A compact UWB antenna with dual band-notch characteristics using nested split ring resonator and stepped impedance resonator," *Microwave and Optical Technology Letters*, Vol. 55, No. 12, 2827–2830, 2013.
13. Luo, X., H. Qian, J.-G. Ma, and E.-P. Li, "Wideband bandpass filter with excellent selectivity using new CSRR-based resonator," *Electronics Letters*, Vol. 46, No. 20, 1390–1391, 2010.
14. Baena, J.-D., "Equivalent-circuit models for split-ring resonators and complementary split-ring resonators coupled to planar transmission lines," *IEEE Transactions on Microwave Theory and Techniques*, Vol. 53, No. 4, 1451–1461, 2005.
15. Bonache, J., M. Gil, I. Gil, J. Garcia-Garia, and F. Martin, "On the electrical characteristics of complementary metamaterial resonators," *IEEE Microw. Wireless Compon. Lett.*, Vol. 16, No. 10, 543–545, 2006.